# The role of motion capture in an illusory transformation of optic flow fields

**Jacob Duijnhouwer**

Functional Neurobiology, Helmholtz Institute,
Utrecht University, Utrecht,
The Netherlands

**Richard J. A. van Wezel**

Functional Neurobiology, Helmholtz Institute,
Utrecht University, Utrecht,
The Netherlands

**Albert V. van den Berg**

Functional Neurobiology, Helmholtz Institute,
Utrecht University, Utrecht,
The Netherlands

In the optic flow illusion, the focus of an expanding optic flow field appears shifted when uniform flow is transparently superimposed. The shift is in the direction of the uniform flow, or "inducer." Current explanations relate the transformation of the expanding optic flow field to perceptual subtraction of the inducer signal. Alternatively, the shift might result from motion capture acting on the perceived focus position. To test this alternative, we replaced expanding target flow with contracting or rotating flow. Current explanations predict focus shifts in expanding and contracting flows that are opposite but of equal magnitude and parallel to the inducer. In rotary flow, the current explanations predict shifts that are perpendicular to the inducer. In contrast, we report larger shift for expansion than for contraction and a component of shift parallel to the inducer for rotary flow. The magnitude of this novel component of shift depended on the target flow speed, the inducer flow speed, and the presentation duration. These results support the idea that motion capture contributes substantially to the optic flow illusion.

## Introduction

In the optic flow illusion (OFI), the focus of a radially expanding pattern of moving dots appears shifted when another pattern of dots that move in one direction is transparently superimposed (Duffy & Wurtz, 1993). This illusory shift is in the direction of the superimposed uniform flow. Studies of the OFI have focused on two alternative explanations for this effect.

One explanation relates the OFI to self-motion and eye movements. Patterns like the expanding radial flow field are thought to be used by the visual system to help guide locomotion since the focus of expansion (FOE) of such fields coincides with the direction of heading (Gibson, 1950). However, smooth pursuit eye movements distort flow fields by adding a component of motion and may hamper the extraction of heading parameters. Specifically, smooth pursuit shifts the retinal location of the FOE in the direction of pursuit (Koenderink & van Doorn, 1987; Longuet-Higgins & Prazdny, 1980). However, evidence exists that the visual system actively compensates for the effects of smooth pursuit from psychophysics (e.g., Royden, Banks,

& Crowell, 1992; van den Berg, 1996; Warren & Hannon, 1990) and electrophysiology (Bradley, Maxwell, Andersen, Banks, & Shenoy, 1996; Lee, Pesaran, & Andersen, 2007; Shenoy, Bradley, & Andersen, 1999; Shenoy, Crowell, & Andersen, 2002; Zhang, Heuer, & Britten, 2004). This smooth pursuit compensation mechanism shifts the perceived FOE location back toward the direction of heading and is thought to operate on the basis of efference copies of pursuit commands and reafferent, purely optical signals (for a review, see Lappe, Bremmer, & van den Berg, 1999). Duffy and Wurtz (1993) hypothesized that the uniform flow field in the OFI is interpreted by the visual system as a reafferent signal indicating smooth pursuit in the opposite direction, thus triggering the compensatory FOE shift. This compensation would perceptually shift the FOE in the direction of the uniform flow: the OFI.

Alternatively, the OFI has been explained by motion induction (MI), the illusory motion of a visual stimulus in the direction opposite to that of the motion of other stimuli (Duncker, 1929; Reinhardt-Rutland, 1988). The uniform flow in the OFI may act as a motion inducer (Meese, Smith, & Harris, 1995). Indeed, subtracting the uniform flow from the radial flow pattern qualitatively explains the

Received October 16, 2007; published April 25, 2008

FOE shift. Several studies have investigated the role of MI in the OFI, focusing on the distinction between local and global MI. Local MI occurs in nearby stimuli and is thought (e.g., Anstis & Reinhardt-Rutland, 1976) to be mediated by antagonistic center-surround interactions in the receptive fields of motion sensitive neurons (Born, 2000; Bridgeman, 1972; Hammond & MacKay, 1981). The OFI has been reproduced in a numerical model of an array of this kind of motion detectors (Royden & Conti, 2003). Global MI, on the other hand, acts on the entire visual field and has been related to cancellation of eye-movements (Lott & Post, 1993; Post, 1986; Post & Heckmann, 1986), shifts in the subjective straight ahead (Brosgole, 1968; Post & Heckmann, 1986), visual–vestibular interactions (Post, 1986; Post, Shupert, & Leibowitz, 1984), and illusory self-motion or vection (Heckmann & Howard, 1991). This class of effects may be more akin to the smooth pursuit compensation hypothesis of the OFI, and it has been argued that global MI might be the mechanism by which the OFI comes about (Pack & Mingolla, 1998). The role of global effects in the OFI has been demonstrated in experiments manipulating the relative sizes (Pack & Mingolla, 1998) and positions (Duijnhouwer, Beintema, van den Berg, & van Wezel, 2006) of the two flow fields.

The OFI is reminiscent of a class of visual illusions in which motion of one stimulus component influences the perceived position of another component. For example, a red square on an equiluminous green background appeared displaced in the direction of drift of overlapping black dots. This "inappropriate binding of motion from one stimulus component to another" occurs in many stimulus configurations and is termed "motion capture" (Ramachandran, 1987). Similar observations have been made by other authors. Spillmann and Redies (1981), for example, noticed that the illusory contours that appear between the ends of dark line segments in a modification of the Ehrenstein (1941) brightness illusion could be captured and dislodged by drifting dots. Possibly related to these effects are the observations that the stationary edges of random dot kinematograms (e.g., Chung, Patel, Bedell, & Yilmaz, 2007; Ramachandran & Anstis, 1990) and moving Gabors (e.g., Arnold, Thompson, & Johnston, 2007; De Valois & De Valois, 1991) perceptually shifted in the direction of the stimuli's internal motion. As a final example (most similar to the OFI), in a stimulus consisting of two random dot patterns, one drifting, and one under a Gaussian luminance envelope, the luminance-defined peak was perceptually displaced in the direction of the moving pattern (Mussap & Prins, 2002).
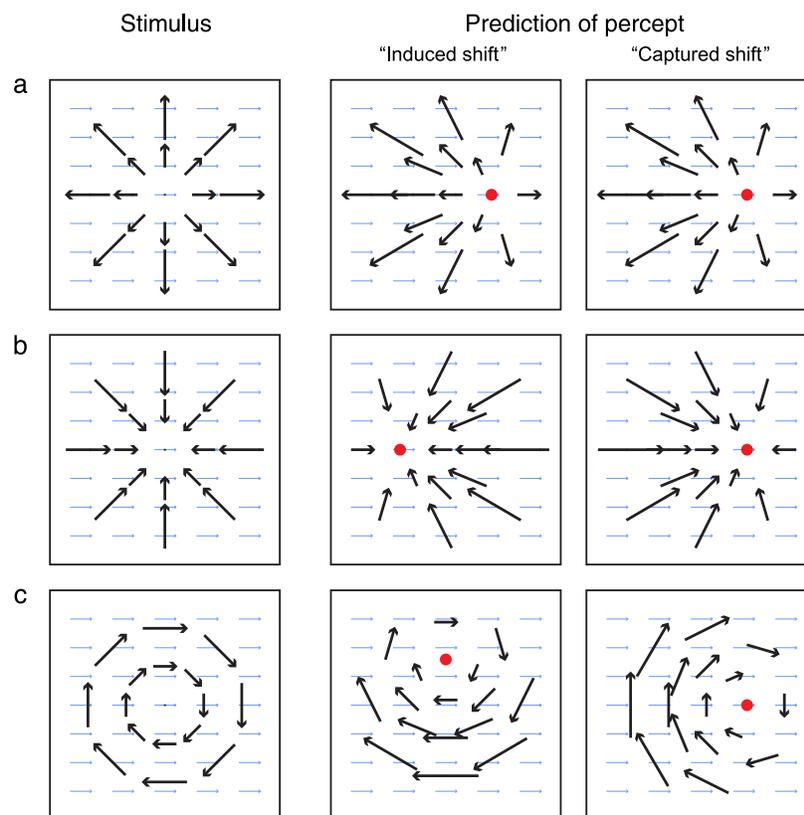


Figure 1. Cartoons of the stimulus conditions (left column) and predictions of the perceived focus position (red dots) based on the pursuit compensation and motion induction accounts (induced shift, middle column) and the alternative explanation based on motion capture of the focus (captured shift, right column). Black arrows indicate target flow. Blue arrows indicate the inducer. Induced shifts should be in the direction of the inducer in expanding flow (a), in the opposite direction in contracting flow (b), and in a perpendicular direction in rotary flow (c). In contrast, captured shifts should be in the direction of the uniform flow in all conditions.

The similarities, in construction and phenomenology, between the OFI and the motion capture illusions suggest that they might be related. Potentially, inappropriate binding of the uniform flow field's motion to the stationary FOE might explain or contribute to the OFI. The purpose of this study is to investigate this third explanation of the OFI. To disentangle the potential contributions to the OFI of, on the one hand, pursuit compensation and motion induction and, on the other hand, motion capture, we here extend the experiment of Duffy and Wurtz (1993) by replacing the expanding flow field with contracting, clockwise, and counterclockwise flow. The expected shift directions of the foci of these flow fields are different in the pursuit compensation and motion induction explanations compared to the explanation based on the capture of the focus by the superimposed uniform flow (Figure 1). For brevity, we will refer to the shifts expected on the basis of pursuit compensation and motion induction as induced shifts in the remainder of this text, whereas shifts in the direction expected on the basis of motion capture will henceforth be called captured shifts. If the OFI is the result of induced shift, the focus of contraction (FOC) should shift in the opposite direction of the uniform flow, instead of shifting in the direction of uniform flow

like the FOE does. Furthermore, a focus of rotary flow should shift perpendicular to the uniform flow (Pack & Mingolla, 1998). In contrast, a captured shift should always be in the direction of the inducing flow field, regardless of the flow condition.

## Methods

### Subjects

In total, eleven subjects participated in the experiments described in this paper. One of them was an author (JD), the others were unaware of the question under research. All subjects had normal vision. Most were experienced psychophysical observers, except for subjects GT and JF, who had no prior experience in psychophysics.

### Visual stimuli

Visual stimuli (Figure 2), subtending $700 \times 700$ pixels, or $74° \times 74°$ at a viewing distance of 104 cm, were
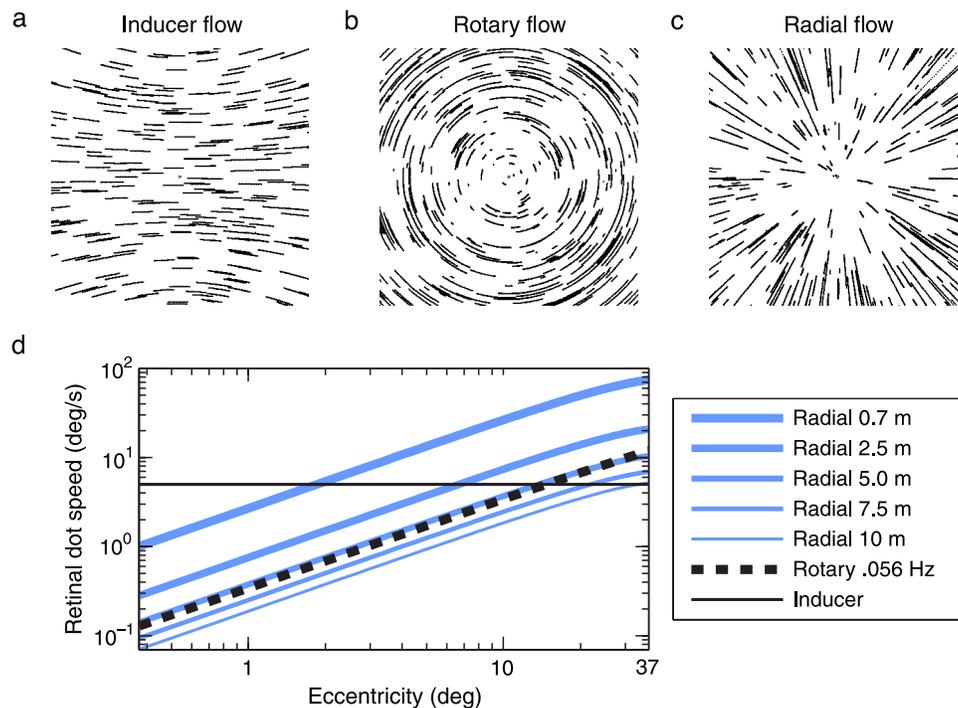


Figure 2. Stimuli consisted of a flow field of horizontally moving dots, or inducer (a), that transparently overlapped either a rotary (b) or a radial target flow field (c). Flow fields were created by simulating rotary and translational observer movements within a scene of dots: a constant yaw of 5°/s in panel a, a pure roll at 0.056 Hz in panel b, and a straight ahead translation at 1.9 m/s in panel c. Note that from the vantage point of the observer, the curved trajectories in panel a resulted in a uniform retinal flow field. In panel d, the retinal velocities of the dots in these three flow fields are shown as a function of eccentricity. The inducer speed is constant across the visual field (solid black line). The retinal speeds in the rotary (dashed black line) and radial (blue lines) flow fields increased with eccentricity. In the radial flow fields, the retinal velocity of a dot decreased with increasing simulated distance from the observer. These distances ranged from 0.7 (thickest blue line) to 10 meters (thinnest blue line).

generated using OpenGL on an Apple PowerMac G4 and back projected onto a translucent screen with a JVC DLA-S10 projector at 75 frames/s. No lighting other than the projector was present in the room. The stimuli consisted of two independent sets of moving dots that were transparently superimposed. Each set provided an optic flow field that simulated a particular observer movement. Of both sets, about 150 dots were visible. The dots had a diameter of 4 pixels (corresponding to 0.5°) and were rendered using OpenGL's anti-aliasing to get smooth animation. A fixation dot, a white square (0.87°) with a black center (0.37°), was visible at the center of the screen. Luminance of the dots, fixation square, and pointer (see Experimental procedure) was 19.6 cd m$^{-2}$ on a 0.08 cd m$^{-2}$ background). Viewing was binocular.

The inducing uniform flow field (henceforth: the inducer) consisted of dots that were randomly positioned on the surface of a sphere (radius 5 m), concentric with the vantage point of the observer. This sphere rotated at 5°/s about a vertical axis through the vantage point or was static.

For the focus carrying flow field, or target flow, the dots were randomly positioned in a volume 15.1 m wide, 15.1 m high, and 9.3 m deep. This volume was centered on a point 5.35 m straight ahead of the observer. Here, the dot motion simulated observer translation along, or rotation about, one of 25 motion axes that were laid out in a 20° × 20° raster, with 5° intervals, centered on the fixation direction. In the rotary OFI experiments, the spin rate varied between 0.02 and 0.28 Hz. In the radial OFI, the magnitude of the simulated translation speeds ranged from 1.13 to 11.3 m/s. The retinal dot speeds caused by these ego-speeds are exemplified in Figure 2d. For the rotary flow (dashed line), the speed of a dot is determined by the product of the spin rate and the sine of the dot's eccentricity. In the radial flow fields, the dot speed additionally depends on the simulated depth of the dot in the scene. The dot speed as a function of eccentricity at five different depths is shown in Figure 2d, with solid blue lines of varying width. The mean dot speed at a given eccentricity is approximately equal to the speed of a dot at three-quarters of the furthest simulated distance in the scene (7.5 m line in Figure 2d). Dots that, due to forward or backward observer translation, passed through the near or far side of the volume were wrapped to the other side of the volume and were assigned new random horizontal and vertical coordinates. Because of this, the dot density was constant during the trial, irrespective of whether the simulated observer motion was forward or backward.

## Experimental procedure

Subjects were seated 104 cm in front of the center of the screen. Their head position was stabilized by means of a biteboard. At the start of each experiment, the participants were familiarized with the stimulus and the task by performing a number of practice trials. Rotary and radial target flow fields were shown in separate sessions.

Each trial consisted of an animation and a pointing phase, the onsets of which were accompanied by auditory cues. A trial started with the animation phase in which the two transparent optic flow displays were simultaneously shown. Subjects were instructed to maintain fixation on the central fixation square and to locate the focus of the target flow. After 1.33 seconds, the flow fields were removed and a pointer (a 0.5° square) appeared centrally on the screen. The subjects were asked to align this pointer with the remembered position by means of a mouse, while maintaining fixation. A mouse click confirmed the position and, after a delay of 107 ms, started the next trial.

## Results

### Two-dimensional illusory focus shifts in radial and rotary flow

We measured horizontal and vertical localization errors of the focus of radial and rotary target flow under influence of transparently superimposed inducer flow. In these optic flow illusion (OFI) experiments, one speed of focus carrying target flow was used. Target flow speed in the radial OFI corresponded to a simulated ego-translation of 3.75 m/s. In the rotary OFI, the target flow simulated a 0.08-Hz roll. Figure 3 is an example of the data of one subject in the rotary flow condition (top row: clockwise flow, bottom row: counterclockwise flow). In these plots, markers represent the mean positional judgments made per veridical focus location. Marker colors indicate the inducer condition: white for leftwards, blue for static, and black for rightwards flow. Error bars represent standard deviations. The horizontal and vertical coordinates of the real and indicated focus positions were analyzed separately (left column: vertical; right column: horizontal). As can be read from the vertical offsets between the data points of the three inducer conditions, the motion of the inducer influenced focus position judgments. The horizontal uniform flow evoked about 3° of vertical shift of the perceived location of the focus for clockwise (Figure 3a) and counterclockwise (Figure 3c) flow. These shifts were up or down, depending on the direction of the inducer and on the direction of rotation of the target flow. These results are in accordance with the pursuit compensation and motion induction accounts of the OFI (Figure 1c, induced shift). However, as can be seen in Figures 3b and 3d, perceptual shifts also occurred in the horizontal direction. These shifts, of about 1.5° in magnitude, were always in the direction of the uniform inducer, irrespective of the sign of the rotation, as predicted by the motion capture account (Figure 1c, captured shift).
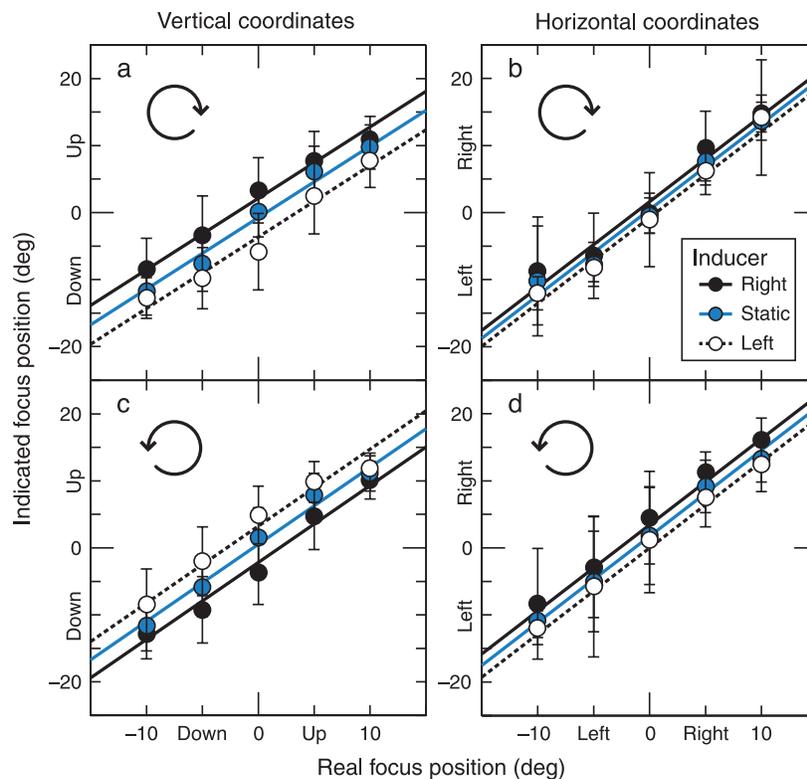
Figure 3. Data of one subject (JD) in the optic flow illusion experiment with rotary target flow. The mean vertical (left column) and horizontal (right column) coordinates of the perceived focus position are plotted against the real coordinates of the focus. Error bars indicate standard deviations. Three inducer conditions were used: rightwards (black), static (blue), and leftwards (white). Circular arrows indicate target flow rotation direction. Vertical shifts could be observed (left column). The focus of clockwise flow appeared higher when the inducer moved rightwards and lower when the inducer moved leftward (a). The vertical shift directions were reversed when the target flow rotated counterclockwise (c). Horizontal shifts were also observed (right column). The horizontal shifts were in the direction of the inducer, irrespective of the rotation direction of the target flow field.

A more formal quantification of the illusory focus shifts in this experiment was achieved by least squares fitting the following planar regression model to the real and indicated focus locations (separately for the horizontal and vertical coordinates):

$$L_i = \alpha + \beta L_r + \gamma V. \qquad (1)$$

Here, $L_i$ is the location that the observer indicated, $L_r$ is the real focus location, and $V$ is the speed of the inducer. This plane was fit separately to the subsets of (unaveraged) data corresponding to each panel in Figure 3. The fit lines in each panel in Figure 3 correspond to cross sections of this plane at 5, 0, and −5°/s inducer speeds $V$ used in this experiment.

All illusory shift values and error ranges that are presented throughout this paper are the estimates and 95% confidence bounds of $\gamma$, obtained by fitting Equation 1, multiplied with the magnitude of the inducer speed $V$ used in the experiment in question. The direction of the shift is indicated by the sign. In the horizontal direction, a positive value signifies that the shift was in the direction of the inducer, and a negative value signifies that the shift

was opposite to the inducer direction. In the vertical direction, positive values signify shifts in a direction 90° away from the inducer direction in the counterclockwise direction. Negative vertical shifts are directed 90° away from the inducer direction in the clockwise direction.

The results of five naive subjects (black markers) and an author (blue markers) that participated in the rotary OFI experiment are shown in the left column of Figure 4. Illusory focus shifts could be observed in all of them, both in the horizontal (Figure 4a) as in the vertical (Figure 4c) direction. Of these six subjects, the mean horizontal shift was 1.60° for the focus of clockwise (FOCW) flow and 1.54° for the focus of counterclockwise (FOCCW) flow. These shifts were statistically significant per subject because zero shift falls outside all 95% confidence intervals. Significant vertical shifts (Figure 4c) were also observed: the mean FOCW shift was 4.00°; the mean FOCCW shift was −3.48°. A negative vertical shift means that the focus shifted downward when the inducer moved to the right and up when the inducer moved to the left. Shifts did not differ significantly between the FOCW and the FOCCW conditions (two-sided sign test: horizontal $p = 1$, $n = 6$; vertical $p = .39$, $n = 6$). Mean per subject
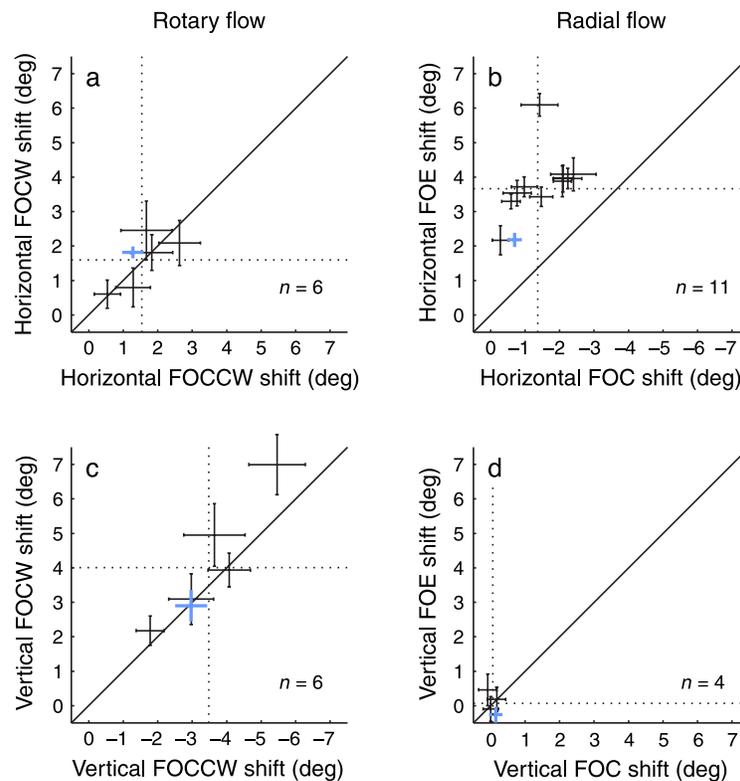
Figure 4. Horizontal and vertical shifts of the foci of contracting and expanding flow fields (right column) and clockwise and counterclockwise flow (left column) per subject with 95% confidence intervals. Positive shift values in the horizontal shift plots a and b indicate shifts in the inducer direction. In the vertical shift plots c and d, positive values indicate shifts at an angle of 90° in the counterclockwise direction with respect to the inducer direction. Note that the abscissas in panels b and c are negative. (a) In the rotary OFI, significant horizontal shifts could be observed in the direction of the inducer in all six observers. Mean shifts (indicated with dashed lines) were 1.60° and 1.54° for the clockwise and counterclockwise flow, respectively. (c) Significant vertical shifts were also observed in all observers, means were 4.00° and −3.48° for the clockwise and counterclockwise flow, respectively. (b) The focus of expanding and contracting flow shifted horizontally in all eleven participants. The shift of the FOE (mean 3.67°) was significantly larger than the shift magnitude of the FOC (mean −1.37°) in all subjects. (d) Vertical shifts were negligible. Data highlighted in blue are from one observer (JD). This subject's data in panels a and c correspond to the data shown in Figure 3.

ratio between horizontal and vertical shifts in this experiment was 42% ± 8% standard deviation.

Ten naive subjects (black markers) and an author (blue marker) participated in the radial OFI experiment. The horizontal focus shifts are shown in Figure 4b. The FOE shifted in the direction of the inducer, and the FOC shifted in the opposite direction. Interestingly, the magnitudes of the FOE shifts were significantly larger than those of the FOC shift (two-sided sign test: $p < 0.001$, $n = 11$). The mean FOE shift was 3.67°; the mean FOC shift was −1.37°. Vertical focus shifts were negligible in the radial OFI (Figure 4d). Note that in this radial OFI experiment, more data are available on the horizontal than on the vertical shifts. Seven subjects took part in an experiment that only required horizontal localization of the FOCs and FOEs (by means of a mouse pointer that was a vertical line spanning the height of the screen) instead of the two-dimensional localization employed in the rest of this study.

Summarizing the results thus far, we found both induced shifts and captured shifts. This was most clearly demonstrated by the rotary OFI. Here, the focus shifted both vertically, as predicted by the pursuit compensation and motion induction accounts, and in the direction of the horizontal inducer flow, as expected on the basis of motion capture. In the radial OFI, we also found induced shifts and captured shifts. As predicted by the pursuit compensation and motion induction accounts, the FOE shifted in, and the FOC shifted opposite the inducer direction. However, the finding that the magnitudes of the FOE shifts were larger than the magnitudes of the FOC shifts suggests that this induced shift was offset by an additional component of shift in the direction predicted by motion capture. For a comparison of induced shifts and captured shifts in rotary and radial flow, see Appendix A.

## Effect of target flow speed

Having identified captured shift as a novel component of the OFI, we wondered how this component would be

influenced by the speed of the target flow. Hence, two-dimensional shifts of radial and rotary target flow foci were measured with two naive subjects (AH and JF) and an author (JD) using a range of target flow speeds.

In the rotary OFI experiment, the spin rates ranged from 0.02 to 0.28 Hz. In the radial OFI experiment, the simulated heading speeds ranged from 1.13 to 11.3 m/s. The inducer speed was 5, 0, or −5°/s. As shown in Figure 5, the horizontal and the vertical shifts in degrees (obtained by fitting Equation 1 to the pointing data and multiplication of $\gamma$ and absolute $V$) varied with the speed of the target flow.

In the rotary OFI (Figure 5a), vertical shifts (diamonds) were observed over the range of spin rates used. The vertical shifts were largest when the target flow speed was

low, reaching almost ±15° in subjects AH and JF. At high absolute spin rates (>0.2 Hz), the shifts were negligibly small. The sign of the shift depended on the rotation direction. The focus of clockwise flow shifted up with the rightward inducer and down with the leftward inducer present. The shift directions were reversed in the counter-clockwise flow condition. These "vertical shift as a function of target speed" data were fit with the hyperbolic function

$$Y = a_y + b_y R^{-1}, \tag{2}$$

where $Y$ is the vertical shift and $R$ is the spin rate. This function reflects the idea of vector subtraction of the uniform flow from the rotary flow because at increasing $R$,
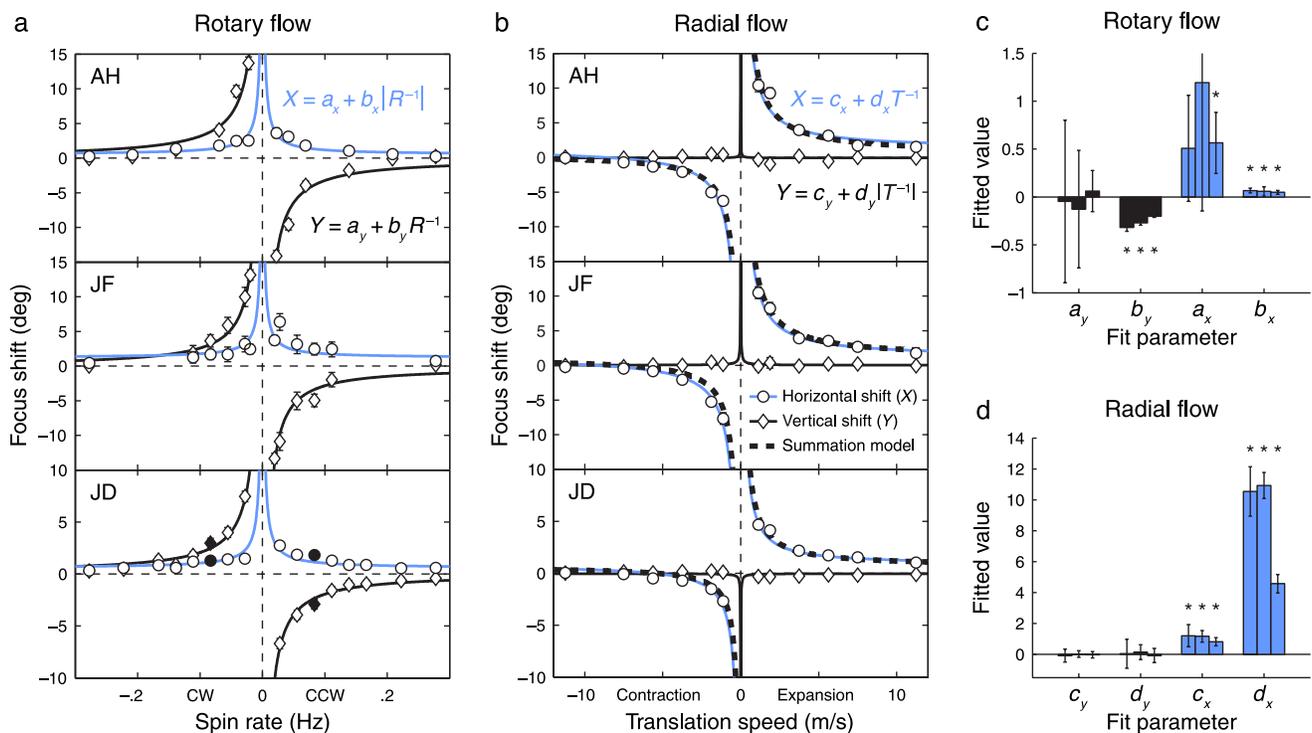


Figure 5. Target flow speed dependence of the horizontal (○) and vertical (◇) focus shifts in the rotary OFI (a) and the radial OFI (b) in three participants (rows). The horizontal axes represent the speed of the target flow, expressed in spin rate (Hz) for the rotary flow, and simulated translation speed (m/s) in the radial flow conditions. Positive horizontal shift values indicate shifts in the direction of the inducer. Positive vertical shift values indicate shifts at an angle of 90° in the counterclockwise direction with respect to the inducer direction. Each shift is collected with inducer speeds of 5, 0, and −5°/s. In the rotary OFI (a), horizontal inducer motion caused vertical shifts (◇) in all subjects. These shifts were positive in clockwise flow and negative in counterclockwise flow. Significant horizontal shifts (○) were also observed in all participants. Both the vertical and the horizontal shifts were greatest at low target flow speeds. This comes to expression also in bar graph (c), which shows the parameters obtained by fitting Equation 2 to the vertical shifts and Equation 3 to the horizontal shifts. The parameters $b_y$ and $b_x$ from the spin rate $R$ term are significantly non-zero in all three subjects, whereas the offsets $a_y$ and $a_x$ are significantly non-zero in only one case. This indicates that both horizontal and vertical shifts in the rotary OFI depend on target flow speed. In the radial OFI (b), the indicated focus positions of expanding and contracting flow were not biased in the vertical direction (◇). Horizontal shifts, however, did occur (○). Here too, shifts were largest at low target flow speeds. Offset $c_x$ is significantly non-zero in all participants (d), meaning that the horizontal shift of the FOE was larger than the shift of the FOC. The dashed line in panel b fitted to the horizontal radial focus shifts is the sum of Equations 2 and 3 that were fitted to rotary flow shifts in panel a, see Appendix A for details. Bars per parameter in panels c and d correspond from left to right to participants in panels a and b from top to bottom. All error bars are 95% confidence intervals. The filled black markers correspond to the data in Figure 3.

the rotary flow vectors are decreasingly influenced by the relatively small uniform flow field vectors, resulting in small vertical shifts $Y$. At near zero spin rates $R$, $Y$ goes asymptotically to plus and minus infinity. This is no problem because the flow field has no focus when the spin rate is zero.

The horizontal shifts (circles in Figure 5a) were positive across the range of spin rates used in all subjects, meaning that they were in the direction of the inducer in both the clockwise and the counterclockwise rotary flow conditions. Here too, the shifts were largest (typically about 3°) at low target flow speeds. We fitted these data with the function

$$X = a_x + b_x|R^{-1}|. \tag{3}$$

The dependence on absolute $R$ reflects the horizontal shift's independence of the direction of rotation. This function also captures the observed diminishing of the horizontal shifts at high spin rates and the increase at lower rates.

Parameter values, with 95% confidence intervals, for the fits to the vertical and horizontal shifts in the rotary flow condition are shown in Figure 5c. The vertical offset $a_y$ was negligible in all observers. And although the horizontal offset $a_x$ ranged from about one half to one degree, it was significant in one subject (JD) only. On the other hand, the spin rate term parameters $b_y$ and $b_x$ were significantly non-zero in all observers, emphasizing the influence of target flow speed on both the vertical and the horizontal illusory focus shifts in the rotary OFI.

Next, we measured the illusory focus shifts in the radial OFI (Figure 5b). We found that shifts were only observed in the horizontal direction, and that the focus of contraction (FOC) shifted less than the focus of expansion (FOE). Vertical offsets were analyzed by fitting the function

$$Y = c_y + d_y T^{-1}, \tag{4}$$

where $T$ denotes translation speed in m/s. The values obtained for $c_y$ and $d_y$ are negligibly small in all three subjects (Figure 5d), which indicates that no mislocalization occurred in the vertical direction.

In the horizontal direction, on the other hand, focus shifts did occur. These were fitted with the function

$$X = c_x + d_x T^{-1}. \tag{5}$$

Large values of $d_x$ indicate that observers experienced large illusory shifts, especially in slowly contracting and expanding flow fields. (Note that the magnitudes of the gain parameters $d$ and $b$ cannot be directly compared, see Appendix A.) Interestingly, the values of $c_x$ are significantly greater than zero in all three observers (mean

$1.06° \pm 0.12°$ *SEM*). This shows that the illusory FOE shifts were, on average, 1.06° larger than the illusory FOC shifts over the range of speeds used in our experiment.

In summary, the results in Figure 5 show that both the induced shift and the captured shift depend on target flow speed. The lower the target flow speed, the larger the shifts. Concerning the shift direction, the induced shift and captured shift show a different dependence on the sign of the target flow. The induced shift direction depends on the sign of the target flow. In contrast, the direction of the captured shift is identical in clockwise and counterclockwise flow and in expanding and contracting flow.

## Effect of target fuzziness

In the literature, it has been shown that the magnitude of the motion capture effect increases with increasing target fuzziness (Murakami, 1999; Murakami & Shimojo, 1993; Ramachandran, 1987). We hypothesized that the increase of the captured shift found at low target flow speeds in the previous experiment might correlate with the fuzziness of the target. To test this hypothesis, we reanalyzed the data of the target flow speeds experiment (Figure 5). Target fuzziness was defined as the standard deviation $\sigma$ of the residuals of a linear fit to the real and indicated position data obtained in the trials in which the inducer was static. Large $\sigma$ means imprecise localization of the focus of flow: fuzzy targets. The results are shown in Figure 6.

First, we established that with increasing absolute target flow speed, target fuzziness decreased, as expressed by an elevated target localization precision in our subjects. This is shown for the radial OFI in Figure 6a and for the rotary OFI in Figure 6b.

Second, we analyzed the relation between the captured shifts and the target fuzziness (Figure 6c). The captured shift in the rotary OFI is defined simply as the horizontal components of the observed mislocalization. In the radial OFI, the captured shift is the difference between the magnitudes of the FOE shift and the FOC shift divided by two. As is shown, the magnitudes of the captured shifts correlated positively with target fuzziness $\sigma$. Linear regression showed that per degree fuzziness, the captured shift was about two-thirds of a degree in the rotary OFI, and about one-third of a degree in the radial OFI.

These results show that the shift in the direction of the inducer is motion capture-like in the sense that its magnitude increases with increasing target fuzziness.

## Effects of presentation duration and inducer speed

To investigate the temporal properties of the induced shift and the captured shift, a naive subject (WP) and an author (JD) participated in an additional rotary OFI
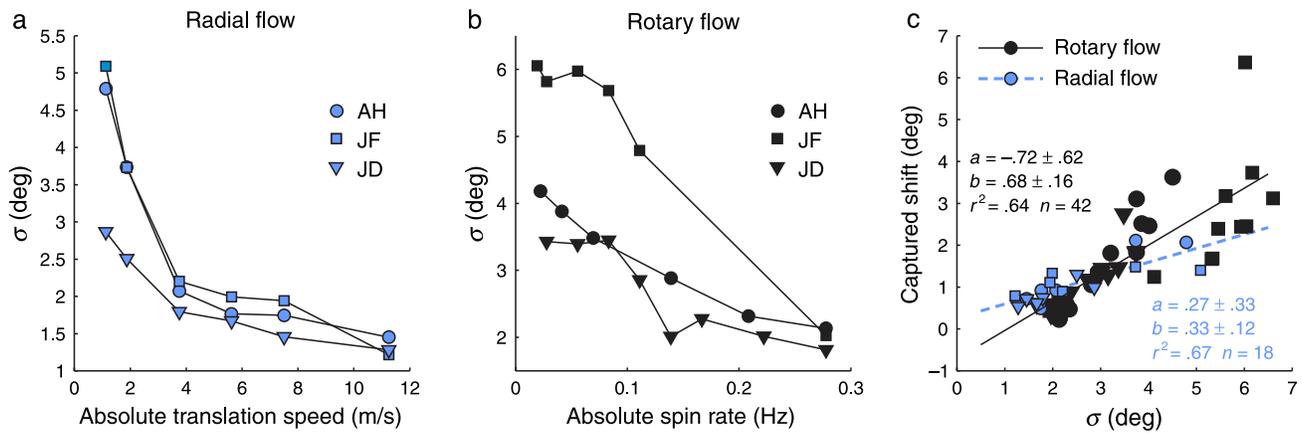
Figure 6. Relation between target fuzziness and captured shift. The fuzziness of the foci of radial (a) and rotary (b) flow is defined as the standard deviation $\sigma$ of localization residuals in the static inducer condition. In all three subjects, $\sigma$ decreased with increasing absolute target flow speed. This means that the focus of faster target flow was more precisely localized. (c) The captured shifts in the rotary and radial OFI increased with target fuzziness. In the rotary flow condition (black markers), the captured shift is defined as the horizontal mislocalization. In the radial flow condition (blue markers), the captured shift is defined as the difference between FOE and FOC shift magnitudes divided by two. Fits are linear regressions of the model Captured shift = $a + b\sigma$.

experiment with variable presentation durations in the range of 0.33 to 5.33 s (Figure 7a). The inducer speed was 5, 0, or $-5°/s$. The spin rate of the target flow in this experiment was 0.08 Hz. Only rotary, not radial, target flow was used because the induced shift and captured shift are most clearly discernable in this condition as vertical and horizontal shifts, respectively.

The horizontal shift increased logarithmically over the range of presentation durations used, reaching 1.6° in subject JD and 4.2° in subject WP. On the other hand, presentation duration did not have an effect on the vertical

shift of the focus. The vertical shifts remained more or less constant at on average 2.7° in subject JD and 6.5° in subject WP.

It has been shown that the magnitude of the OFI increases with increasing inducer speed (Duffy & Wurtz, 1993) before leveling off at even higher inducer speeds (Pack & Mingolla, 1998). We wondered whether this holds for both the induced shift component and the captured shift component. With the same subjects as in the presentation duration experiment, we investigated the effect of inducer speed on the horizontal and vertical focus
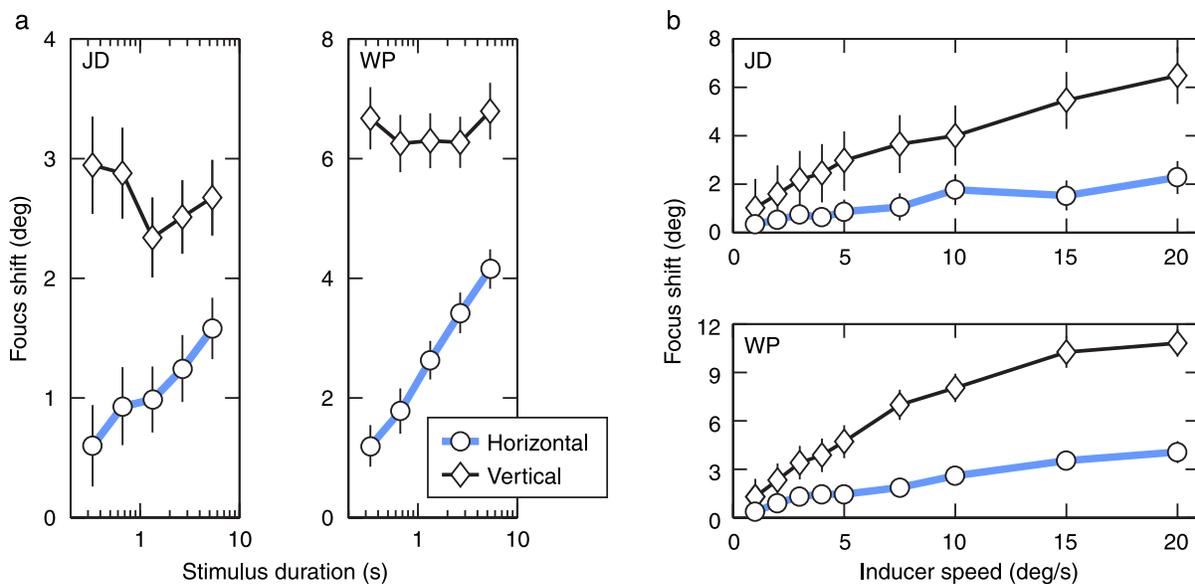


Figure 7. The effect of stimulus duration (a) and inducer speed (b) on the magnitudes of the vertical (◊) and horizontal (○) components of focus shift in the rotary OFI. (a) In both subjects, stimulus duration had no effect on the vertical shifts over the range of durations used. The horizontal shift, however, increased logarithmically with stimulus duration. (b) Both the horizontal and the vertical shifts increased with increasing inducer speed in both subjects, leveling off at higher speeds.

shifts using a constant presentation duration of 1.33 s ([Figure 7b](#)). Spin rate was 0.08 Hz, and the inducer speed ranged from 1°/s to 20°/s. Both shift components show a clear increase over this range, and both level off at higher inducer speeds.

## Effect of eye movements

Although we instructed our subjects to fixate the stationary square at the center of the screen and to avoid tracking of the moving dots, involuntary eye movements might have occurred in our experiments. To confirm whether or not eye movements could contribute or explain our results, we repeated the rotary OFI experiment with three participants while recording their eye movements. Offline analysis showed that, although eye traces did differ slightly amongst leftward, static, and rightward inducer conditions, the eye movements did not correlate with the captured shift in any of the participants. Details on these data and analyses can be found in [Appendix B](#).

# Discussion

We reproduced the optic flow illusion (OFI) in which the focus of an expanding flow field appears shifted in the direction of a transparently superimposed uniform flow field (Duffy & Wurtz, [1993](#)). We then extended the OFI by replacing the expansion pattern with contracting and rotary flow fields. This revealed that there are at least two sources of flow field transformation. On the one hand, the foci of these flow fields shifted in the direction expected on basis of the existing smooth pursuit compensation and motion induction explanation of the OFI ([Figure 1](#), middle column). On the other hand, a component of shift was observed that was always in the direction of the horizontal inducer flow. In the rotary OFI, this newly identified captured shift was separated from the known induced shift effect because the captured shift was horizontal and the induced shift was vertical. In the radial OFI, the effect could be observed as an asymmetry between the magnitudes of the shifts of the foci of expansion and contraction. However, although this asymmetry could be explained on the basis of the isolated captured and induced shifts from the rotary flow conditions ([Appendix A](#)), we cannot exclude other possible contributions to the asymmetry. For example, the reduced shift of the focus of contraction might have been caused by a reduced compensation for pursuit in contracting flow, possibly because contracting flow is under natural locomotor behavior much rarer than expanding flow. In addition, evidence exists for differential processing of expanding and contracting flow in humans (e.g., Holliday & Meese, [2005](#); Lappe & Rauschecker, [1995b](#); Ptito, Kupers, Faubert, & Gjedde,

[2001](#)), which might also be related to the observed asymmetry.

The captured shift could account for a substantial part of the total OFI shift. For example, the captured shift magnitude was 42% of the induced shift magnitude in the 0.08-Hz rotary OFI experiment on average per subject ([Figure 4](#)). This component of the focus shift went unnoticed in other psychophysical studies of the OFI that only used expanding target flow (Duffy & Wurtz, [1993](#); Duijnhouwer et al., [2006](#); Grigo & Lappe, [1998](#); Royden & Conti, [2003](#)). In one study (Pack & Mingolla, [1998](#)), a rotary target flow was used, and although not mentioned by the authors, a capture like shift of comparable magnitude can be discerned in the results. Yet, as the authors used only clockwise flow, it is impossible to establish from their data whether the direction of this shift was independent of the direction of the target flow rotation. Thus, our study for the first time provides a clear distinction between capture and induction components of the optic flow illusion.

We further investigated the isolated induced shift and captured shift components by manipulating the target flow speed, the inducer speed, and the presentation duration. Manipulating the target flow speed had a clear effect on the induced shift ([Figure 5](#)). The slower the target flow, the larger the shift. This makes sense in terms of the smooth pursuit compensation account. Smooth pursuit, adding global motion to the retinal flow field, has the greatest effect when the target flow field vectors are short. Therefore, with slow target flow, the compensation needs to be stronger, hence more illusory shift occurs in the slow target OFI. It has been shown in flow sensitive neurons in the medial superior temporal (MST) cortex area of the macaque that compensation effects for real pursuit are indeed scaled to the speed of the radial flow (Lee et al., [2007](#)).

Manipulating the target flow speed had a similar effect on the captured shift as on the induced shift ([Figure 5](#)). The slower the target flow, the larger the shift. This increase at lower target speeds could be explained by taking into account that the focus of the target flow becomes fuzzier at low flow speeds. We found clear relations between target flow speeds and localization uncertainty on the one hand, and between localization uncertainty and the captured shift on the other ([Figure 6](#)). Other studies have also found positive correlations between target fuzziness and the strength of the motion capture effect. Optimum motion capture has been found in target stimuli with low luminance or color contrast, smaller size, and greater eccentricity (Murakami, [1999](#); Murakami & Shimojo, [1993](#); Ramachandran, [1987](#)). Targets that by manipulation of these parameters ranged from fuzzy to distinct allowed a gradual change from motion capture to motion induction (Murakami, [1999](#); Murakami & Shimojo, [1993](#)). Likewise, the illusion that the stationary edges of random dot kinematograms (Ramachandran & Anstis, [1990](#)) and moving Gabors

(De Valois & De Valois, 1991) shift in the direction of the stimuli's internal motion was optimal when those edges were least conspicuous, e.g., when they were hidden in a surround of static dots or under a luminance envelope (Chung et al., 2007). Our results show that the OFI stimulus provides an additional method of manipulating target fuzziness by means of the target flow speed.

Increasing the inducer speed had similar effects on the induced shift and the captured shift (Figure 7b). Both shifts showed a saturating increase with increasing inducer speed, similar to the inducer speed dependence of the expansion OFI found in a previous study (Pack & Mingolla, 1998). Manipulating the stimulus duration, however, revealed different temporal properties of the induced shift and the captured shift (Figure 7a). Manipulating the stimulus duration (0.33–5.33 s) did not have an effect on the magnitude of the induced shift (Figure 7a). One might have expected such an effect when the buildup of pursuit compensation or motion induction is ongoing. The absence of an effect of stimulus duration implies short buildup times of motion induction and pursuit compensation relative to the shortest presentation duration used in our experiment. However, the literature on the buildup times of local motion induction and smooth pursuit compensation is mixed.

Local motion induction might indeed be very fast, as it has been shown psychophysically (Tadin, Lappin, & Blake, 2006) and electrophysiologically (Perge, Borghuis, Bours, Lankheet, & van Wezel, 2005) that the surround modulates the response of center-surround motion detectors after a delay of only about 16 ms. However, a related illusion known as motion repulsion, the illusory overestimation of acute angles between the directions of two transparently superimposed uniform flow fields (e.g., Marshak & Sekuler, 1979), has been shown to increase over a range of presentations durations similar to the ones used in Figure 7a (Rauber & Treue, 1999). Since motion repulsion is thought to be related to center-surround motion interactions (e.g., Hiris & Blake, 1996; Marshak & Sekuler, 1979) and since applying motion repulsion to any location within the OFI stimuli qualitatively explains the induced shift, these findings seem incongruous with the lack of effect of stimulus duration on induced shift reported here. However, the buildup of motion repulsion in the study of Rauber and Treue (1999) might have been due to local motion adaptation, which may have had a less prominent role in our experiments because of the relatively low dot density used.

In terms of pursuit compensation, the finding that the Filehne (1922) illusion (the illusory motion of a dot in total darkness because of incomplete compensation for the eye movements of the observer) disappears after about 200–300 ms (de Graaf & Wertheim, 1988; Mack & Herman, 1978) seems to match the constant induced shift over the range of stimulus durations used in our experiment (0.33–5.33 s). However, others have shown that the pursuit compensation can continue to build for at least a

second (Souman, Hooge, & Wertheim, 2005). Moreover, it is important to note that these durations were found for extraretinal compensation during real pursuit. To our knowledge, no study has quantified the latency of pursuit compensation based on purely retinal signals.

As opposed to the induced shift, manipulating the stimulus duration did have an effect on the captured shift. The captured shift increased with increasing stimulus duration and saturated at longer presentation times. The increase with longer durations matches the idea of target drift caused by motion capture instead of a fixed magnitude, quasi-instantaneous shift. The captured shift might saturate over time because an equilibrium sets in between the offsetting motion signal and the veridical position signal.

## Comparison of stimuli with previous studies

Apart from the additional contracting and rotary flow conditions, the OFI stimuli used in this study differed in a number of ways from those used by Duffy and Wurtz (1993) and other studies of the OFI.

First, in all experiments in this study, a fixation dot was permanently visible at the center of the screen. This is different from most previous studies, which lacked a fixation dot during the stimulus presentation intervals (Grigo & Lappe, 1998; Pack & Mingolla, 1998; Royden & Conti, 2003). The stationary fixation marker might have had a detrimental effect on the illusory shift. Since a fixation marker provides visual evidence against ongoing pursuit, it may counteract a pursuit-compensation mechanism. However, the induced shifts reported here are of the same order of magnitude as in previous studies, supporting an earlier claim (Duffy & Wurtz, 1993) that fixation does not influence the illusory shift much.

Second, our inducer flow stimulus was constructed by simulating an eye-rotation within a sphere of dots. This resulted in curved dot trajectories on the display and a uniform flow field on the retina of the observer. In contrast, the inducers in previous studies of the OFI (Duffy & Wurtz, 1993; Grigo & Lappe, 1998; Pack & Mingolla, 1998; Royden & Conti, 2003) consisted of dots moving with uniform velocity on the display, in effect simulating sideways observer translation along a frontoparallel plane. Physical differences between stimuli constructed in these alternative ways are most clearly visible in the periphery of large field stimuli, such as used in our experiment (Figure 2). Since it has been suggested that these differences can be used by human observers as cues to decompose combined translational and rotational flow (Grigo & Lappe, 1999), we chose to use the rotational flow inducer as to maximize a potential contribution of an eye-rotation compensation mechanism to the OFI (Duijnhouwer et al., 2006).

Finally, in previous studies the target flow was a frontoparallel plane of dots moving at a speed that scaled

linearly with eccentricity. In contrast, our radial stimuli were created by simulating observer translation through a cloud of dots. Dots were wrapped to the far side of the cloud when they came nearer than 0.7 m to the observer in the expansion condition. In the contraction condition, the dots were wrapped to the near side of the cloud when they exceeded a distance of 10 m away from the observer. Thus, the dot density was kept constant around both the focus of expansion and the focus of contraction, an issue that needs special consideration in studies comparing expanding and contracting flow (cf. Clifford, Beardsley, & Vaina, 1999). An additional result of adding depth to the scene is that, in the radial flow conditions, dots at identical eccentricities could have different speeds (motion parallax). Given the importance of motion parallax in heading tasks that require decomposition of rotational and translational flow (Rieger & Toet, 1985; Warren & Hannon, 1988, 1990), it is interesting to note that the OFI does also occur in radial target flow with simulated depth in the scene. However, because motion parallax was absent in the rotary flow conditions (flow due to rotation around the vantage point is invariant for depth in the scene), the comparison between the illusory shifts observed in radial and rotary flow was more complicated than it would have been when no depth was simulated (Appendix A).

## The mechanism of the captured shift

The effects on the magnitude on the captured shift of target fuzziness and the saturation of captured shift with increasing speed and stimulus duration suggest that the target is dislodged by the inducer and drifts along with it up to the limits set by the distinctness (as a reciprocal of fuzziness) of the target.

More mechanistically speaking, the captured shift might be related to the dynamic spatial remapping of receptive fields that are tuned to our target flow fields. Neurons tuned to radial and rotary flow have been found in many cortical areas, most notably in the medial superior temporal (MST) area of the macaque (e.g., Duffy & Wurtz, 1991, 1995, 1997; Saito et al., 1986; Tanaka et al., 1986) and humans (Dukelow et al., 2001; Goossens, Dukelow, Menon, Vilis, & van den Berg, 2006; Greenlee, 2000; Morrone et al., 2000; Peuskens, Sunaert, Dupont, Van Hecke, & Orban, 2001; Rutschmann, Schrauf, & Greenlee, 2000). Efference copies of oculomotor signals that might be used to shift the receptive fields have been observed in MST (Newsome, Wurtz, & Komatsu, 1988; Goossens et al., 2006). Presumably, the inducer in the OFI stimulates pursuit eye movement neurons, found for example in the frontal eye field (FEF; Gottlieb, Bruce, & MacAvoy, 1993; Gottlieb, MacAvoy, & Bruce, 1994; MacAvoy, Gottlieb, & Bruce, 1991; Tian & Lynch, 1996a, 1996b), a cortical area that has been shown to project onto MST (Stanton, Bruce, & Goldberg, 1995). Although the

stimuli in our experiment were viewed with static eyes (Appendix B), the activity of neurons in the FEF might have been enough to trigger the dynamic receptive field shifts. A similar dynamic field shift due to subthreshold oculomotor signals has been found in macaque V4 and has been related to covert spatial attention shifts (Moore & Armstrong, 2003; Moore & Fallah, 2004; Schall, 2004; Thompson, Biscoe, & Sato, 2005). Motion capture has also been related to attentive tracking (Culham & Cavanagh, 1994), and shifting receptive fields might functionally underpin this idea. Regarding the saturating increase of the captured shift as a function of target fuzziness, we speculate that the shift may be related to neural units with dynamic tuning properties. Models of such dynamic tuning rely on gain-fields, i.e., multiplicative interactions between extraretinal or reafferent pursuit signals and visual receptive fields (e.g., Beintema & van den Berg, 1998; Zipser & Andersen, 1988). The inducer motion presented to a stationary eye causes a mismatch between visual motion and eye movement related dynamic shifts. This mismatch may be perceptually valid within the bounds set by the precision of the representation of the focus. Our measure of target fuzziness ($\sigma$) suggests that the focus of optic flow is represented at a coarser scale as $\sigma$ increases (cf. the relation between diffusion and spatial scale in Koenderink, 1988). When the scale of a model gain-field increases, its limit for dynamic shifting also increases (Beintema & van den Berg, 1998). Thus, a captured shift caused by dynamic tuning may increase as $\sigma$ increases until it is limited at the largest receptive field scale.

## Conclusion

We conclude that the OFI is an addition of at least two separate effects, namely, an induced shift, presumably caused by pursuit compensation and/or motion induction, and a captured shift, which may be caused by an interaction of the motion signal of the inducer and the position signal of the focus. The captured shift magnitude was typically 42% of the induced shift magnitude observed in our experiments. Computational models of the OFI (Hanada, 2005; Lappe & Duffy, 1999; Lappe & Grigo, 1999; Lappe & Rauschecker, 1995a; Royden & Conti, 2003) have been developed without the captured shift component in mind and have been tested with expanding patterns of motion only. The experimental results presented in this study provide new constraints on these models. Therefore, it might prove interesting to see how these models respond to the rotary and contracting flow stimuli used in our experiments. Possibly, the captured shift will appear as an emergent property in one or more of them. Or perhaps the models and the data can be reconciled by modifications to the models that are potentially informative of how the visual system integrates motion and position information.

## Appendix A

### Comparison of radial and rotary focus shifts

In the rotary OFI experiment, the induced shift was perpendicular to the inducer, and the captured shift was parallel to the inducer. In the radial OFI experiment, however, the induced shift and captured shift were parallel and were only discernable as a difference in the magnitude of the FOE and FOC shifts. We can qualitatively explain this shift magnitude difference because the captured shift, being always in the direction of the inducer, strengthens the induced shift of the FOE (that is also in the direction of the inducer) and counterbalances the induced shift of the FOC (that is opposite the inducer).

This idea can be tested more quantitatively by reanalyzing the data of the target flow speed experiment (Figure 5). If the differences between FOE and FOC shift magnitudes in the radial target flow speed experiment are indeed the result of the same captured shifts that are manifest as horizontal shifts in the rotary target flow speed experiment, we would expect that the horizontal shifts of the radial foci can be predicted by the sum of the individual fits to the horizontal and vertical rotary focus shifts. However, this comparison is complicated by the fact that the spin rate and translation speed axes in Figure 5 are not directly comparable. Because of the depth in the virtual environment of dots, the simulated ego-speed (in m/s) translates into a mixture of dot speeds at any given visual direction with dots at greater distances from the observer having lower dot speeds than closer dots (motion parallax). The simulated spin rate (in Hz), on the other hand, translates into a dot speed profile that has a single, linear relation with eccentricity. This difference is illustrated in Figure 2d. In matching the illusory shifts in the radial and rotary conditions, the problem is that the relative contributions of far and close dots to the radial OFI are unknown.

The data does, however, allow for a qualitative consistency check of this prediction. We summed Equations 2 and 3, the two fits to the horizontal and vertical shifts of the rotary flow, yielding

$$X = a_y + b_y R^{-1} + a_x + b_x |R^{-1}|. \tag{A1}$$

To deal with the problem of moving from the domain of spin rates to translation speeds, as explained in the previous paragraph, we substituted the spin rate $R$ by the translation speed $T$ multiplied by a scaling factor $k$ (in m$^{-1}$) resulting in

$$X = a_y + b_y (kT)^{-1} + a_x + b_x |(kT)^{-1}|. \tag{A2}$$

We then fitted this summation model to the horizontal shifts in the radial target flow experiments, keeping parameters $a_y$, $b_y$, $a_x$, and $b_x$ fixed at the values obtained in fitting the focus shift data with Equations 2 and 3, and $k$ as the only free parameter. These fits are shown in Figure 5b as dashed lines. The model fits the observed horizontal shifts well (mean $r^2$ for all subjects is 0.97). The fitted values of $k$ were 0.030, 0.034, and 0.025 for subjects AH, JD, and JF (mean 0.029). This means that the horizontal shifts in a radial OFI at, for example, 1.9 m/s ego-translation were equal to the sum of the horizontal and vertical shifts in the rotary OFI when the spin rate was 1.9 m/s × 0.029 m$^{-1}$ = 0.056 Hz. The spin rate and the translation speed of this example were used in making the flow fields pictograms in Figures 2b and 2c. As shown in the corresponding speed profile plot in Figure 2d, the retinal dot speeds in the 0.056-Hz rotation stimulus are equal to the retinal dot speeds in the 1.9-m/s translation condition of dots at an intermediate distance of about 5 meters from the observer. Note that the mean distance of the visible subset of dots in the volume of dots was about 7.5 meters. That our subjects appear to have judged the focus position on these nearer than average dots seems plausible: these dots moved faster and thus conveyed clearer information on the location of the focus. We think this comparison suggests that the observed difference between FOC and FOE shifts likely result from the same effect that caused the horizontal shifts in the rotary OFI.

## Appendix B

### Eye movements control experiment

Large field moving stimuli, such as the inducer stimuli used in this study, are known to evoke involuntary optokinetic nystagmus (OKN), reflexive eye movements alternating between short pursuit phases and saccades in the opposite direction. Recently, OKN has been shown to cause systematic localization errors (Kaminiarz, Krekelberg, & Bremmer, 2007; Tozzi, Morrone, & Burr, 2007). Although the targets in those studies were brief flashes, a similar phenomenon might occur when localizing persistent targets such as the flow field foci used in this study. Could the focus shifts be explained by involuntary eye movements that our subjects might have made, despite instructions to avoid tracking of the moving dots and maintain fixation? To test this possibility, we repeated the rotary OFI experiment with two naive subjects (WP and GT) and an author (JD) while recording the movements of their left eyes at a sample rate of 500 Hz with a video eye-tracker (Eyelink II; SR Research, Ltd.). Experimental conditions were identical to the first experiment in this paper (Figures 3 and 4a, c).

The control experiment comprised a 9-point Eyelink calibration sequence, followed by 300 trials of clockwise and counterclockwise flow at 0.08 Hz. The inducer moved at ±5°/s or was static. Every tenth trial the subjects fixated a calibration dot, which was used offline to recalibrate the Eyelink signal. These thirty calibration trials were not used for further analysis. Gaze traces were analyzed over the stimulus interval (1.33 s), the first sample of the trace was defined as being at zero degrees eccentricity. Trials in which the gaze trace exceeded 2.5° in the horizontal or vertical direction from the fixation dot were discarded. This occurred, averaged over our three subjects, in 5% of the trials and was mostly due to eye blinks.

Of the localization data of the remaining trials, the horizontal and vertical focus shifts were analyzed by means of fitting the planar regression model Equation 1. To obtain single values for the horizontal and vertical shifts, the counterclockwise flow condition was analyzed as if the target spun clockwise. This was achieved by taking the additive inverse of the veridical and indicated vertical coordinates during counterclockwise flow. The horizontal shift ($X$) and vertical shift ($Y$) values thus obtained are shown in Figure 8a. Significant horizontal (captured) and vertical (induced) shifts could be observed in all three observers and are comparable to the shifts presented in Figures 3 and 4a, c.

In Figure 8b, the horizontal and vertical gaze traces during leftward (red), static (green), and rightward (blue) inducer flow are superimposed for all non-discarded trials. To give an impression of the difference between the
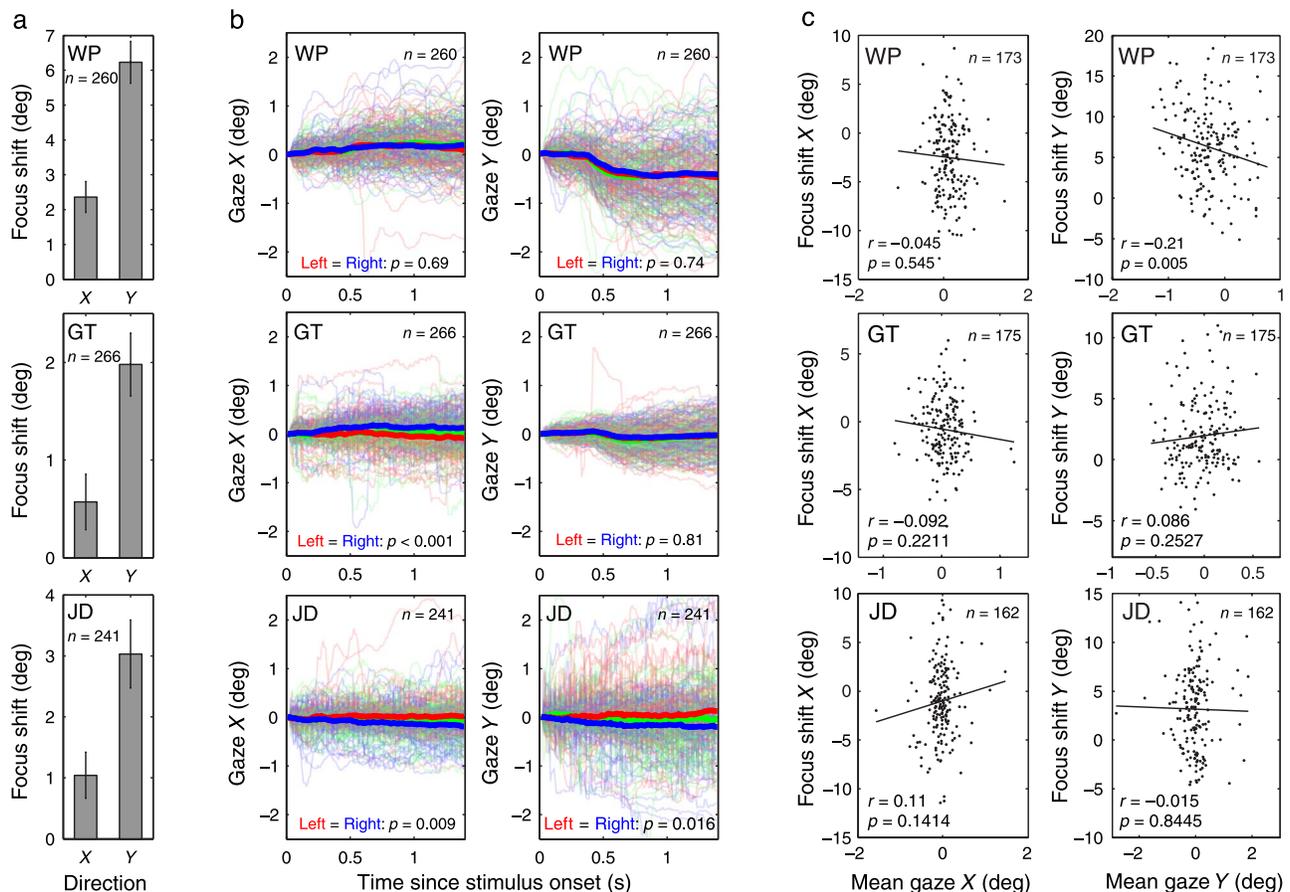


Figure 8. Relation between eye movements and the horizontal and vertical focus shifts observed in three subjects for the rotary target flow experiment. The experimental settings were identical to the experiments of Figure 3 and Figure 4a, c. (a) The horizontal ($X$) and vertical ($Y$) focus shifts of the observed in this control experiment obtained by fitting Equation 1 and multiplying and the magnitude of the inducer speed $V$. These shifts are comparable to shift values in Figures 3 and 4a, c. (b) The horizontal and vertical gaze positions of three subjects (rows) from the onset to the end of each trial. Red, green, and blue traces correspond to trials with leftward, static, and rightward inducing motion, respectively. Thick lines are the mean traces of these three conditions. For statistical analysis, each trace was summarized with the mean gaze position over the course of a trial. The populations of trace means were significantly different between leftward and rightward inducer conditions in all but one of our subjects (Wilcoxon rank sum test, see panel b for $p$-values). However, the correlograms (c) show that the trace means and focus localization errors per trial were uncorrelated, except for one subject (WP) showing a significant correlation between vertical eye movements and vertical biases (induced shift). We conclude that the horizontal (captured) shifts reported in this study are not related to eye movements.

inducer conditions, the mean of all traces recorded in each inducer condition is plotted as a thick line in the corresponding color. Visual inspection of the individual (per trial) gaze traces did not reveal any OKN, which would have resulted in a marked pattern of smooth pursuit phases in the direction of the inducer alternated by rapid saccades back to the fixation dot. However, further statistical analysis in which we reduced each individual gaze trace to a single trace mean value (mean gaze position over the course of the trial) revealed that the population of horizontal trace means recorded during leftward and rightward inducer flow were significantly different in two out of three subjects (Wilcoxon rank sum test, see Figure 8b for *p*-values). However, the absolute differences between mean gaze traces (indicated with thick lines in Figure 8b) are of a much smaller magnitude than the captured shifts observed (Figure 8a). Moreover, as is shown in Figure 8c, correlating the per trial trace means with the per trial mislocalization of the focus revealed no significant correlation between the horizontal eye position and the horizontal focus shifts in any of our subjects. For this correlation, only the trials with a moving inducer were used (hence the lower *n*-values in Figure 8c compared to Figures 8a and 8b), and clockwise and counterclockwise flow trial data were made congruent (as described in the previous paragraph). For completeness, the correlations between the vertical eye positions and the vertical focus shifts are shown in Figure 8c, right column. We conclude from this control experiment that the horizontal captured shifts reported in this study were not related to eye movements.

## Acknowledgments

Commercial relationships: none.
Corresponding author: Jacob Duijnhouwer.
Email: j.duijnhouwer@gmail.com.
Address: H.R. Kruytgebouw, Padualaan 8, NL-3584 CH Utrecht, The Netherlands.

## References

Anstis, S. M., & Reinhardt-Rutland, A. H. (1976). Interactions between motion aftereffects and induced movement. *Vision Research, 16,* 1391–1394. [PubMed]

Arnold, D. H., Thompson, M., & Johnston, A. (2007). Motion and position coding. *Vision Research, 47,* 2403–2410. [PubMed]

Beintema, J. A., & van den Berg, B. (1998). Heading detection using motion templates and eye velocity gain fields. *Vision Research, 38,* 2155–2179. [PubMed]

Born, R. T. (2000). Center-surround interactions in the middle temporal visual area of the owl monkey. *Journal of Neurophysiology, 84,* 2658–2669. [PubMed] [Article]

Bradley, D. C., Maxwell, M., Andersen, R. A., Banks, M. S., & Shenoy, K. V. (1996). Mechanisms of heading perception in primate visual cortex. *Science, 273,* 1544–1547. [PubMed]

Bridgeman, B. (1972). Visual receptive fields sensitive to absolute and relative motion during tracking. *Science, 178,* 1106–1108. [PubMed]

Brosgole, L. (1968). An analysis of induced motion. *Acta Psychologica,* 28:1–44.

Chung, S. T., Patel, S. S., Bedell, H. E., & Yilmaz, O. (2007). Spatial and temporal properties of the illusory motion-induced position shift for drifting stimuli. *Vision Research, 47,* 231–243. [PubMed]

Clifford, C. W., Beardsley, S. A., & Vaina, L. M. (1999). The perception and discrimination of speed in complex motion. *Vision Research, 39,* 2213–2227. [PubMed]

Culham, J. C., & Cavanagh, P. (1994). Motion capture of luminance stimuli by equiluminous color gratings and by attentive tracking. *Vision Research, 34,* 2701–2706. [PubMed]

de Graaf, B., & Wertheim, A. H. (1988). The perception of object motion during smooth pursuit eye movements: Adjacency is not a factor contributing to the Filehne illusion. *Vision Research, 28,* 497–502. [PubMed]

De Valois, R. L., & De Valois, K. K. (1991). Vernier acuity with stationary moving Gabors. *Vision Research, 31,* 1619–1626. [PubMed]

Duffy, C. J., & Wurtz, R. H. (1991). Sensitivity of MST neurons to optic flow stimuli. I. A continuum of response selectivity to large-field stimuli. *Journal of Neurophysiology, 65,* 1329–1345. [PubMed]

Duffy, C. J., & Wurtz, R. H. (1993). An illusory transformation of optic flow fields. *Vision Research, 33,* 1481–1490. [PubMed]

Duffy, C. J., & Wurtz, R. H. (1995). Response of monkey MST neurons to optic flow stimuli with shifted centers of motion. *Journal of Neuroscience, 15,* 5192–5208. [PubMed] [Article]

Duffy, C. J., & Wurtz, R. H. (1997). Planar directional contributions to optic flow responses in MST neurons. *Journal of Neurophysiology, 77,* 782–796. [PubMed] [Article]

Duijnhouwer, J., Beintema, J. A., van den Berg, A. V., & van Wezel, R. J. (2006). An illusory transformation of optic flow fields without local motion interactions. *Vision Research, 46,* 439–443. [PubMed]

Dukelow, S. P., DeSouza, J. F., Culham, J. C., van den Berg, A. V., Menon, R. S., & Vilis, T. (2001). Distinguishing subregions of the human MT+ complex using visual fields and pursuit eye movements. *Journal of Neurophysiology, 86,* 1991–2000. [PubMed] [Article]

Duncker, K. (1929). Über induzierte Bewegung (Ein Beitrag zur Theorie optisch wahrgenommener Bewegung). *Psychologische Forschung, 12,* 180–259.

Ehrenstein, W. (1941). Über Abwandlungen der L Hermannschen Helligkeitserscheinung. *Zeitschrift für Psychologie, 150,* 83–91.

Filehne, W. (1922). Über das optische Wahrnehmen von Bewegungen. *Zeitschrift für Sinnesphysiologie, 53,* 134–144.

Gibson, J. J. (1950). *The perception of the visual world.* Boston: Houghton Mifflin.

Goossens, J., Dukelow, S. P., Menon, R. S., Vilis, T., & van den Berg, A. V. (2006). Representation of head-centric flow in the human motion complex. *Journal of Neuroscience, 26,* 5616–5627. [PubMed] [Article]

Gottlieb, J. P., Bruce, C. J., & MacAvoy, M. G. (1993). Smooth eye movements elicited by microstimulation in the primate frontal eye field. *Journal of Neurophysiology, 69,* 786–799. [PubMed]

Gottlieb, J. P., MacAvoy, M. G., & Bruce, C. J. (1994). Neural responses related to smooth-pursuit eye movements and their correspondence with electrically elicited smooth eye movements in the primate frontal eye field. *Journal of Neurophysiology, 72,* 1634–1653. [PubMed]

Greenlee, M. W. (2000). Human cortical areas underlying the perception of optic flow: Brain imaging studies. *International Review of Neurobiology, 44,* 269–292. [PubMed]

Grigo, A., & Lappe, M. (1998). Interaction of stereo vision and optic flow processing revealed by an illusory stimulus. *Vision Research, 38,* 281–290. [PubMed]

Grigo, A., & Lappe, M. (1999). Dynamical use of different sources of information in heading judgments from retinal flow. *Journal of the Optical Society of America A, Optics, Image Science, and Vision, 16,* 2079–2091. [PubMed]

Hammond, P., & MacKay, D. M. (1981). Modulatory influences of moving textured backgrounds on responsiveness of simple cells in feline striate cortex. *The Journal of Physiology, 319,* 431–442. [PubMed] [Article]

Hanada, M. (2005). Computational analyses for illusory transformations in the optic flow field and heading perception in the presence of moving objects. *Vision Research, 45,* 749–758. [PubMed]

Heckmann, T., & Howard, I. P. (1991). Induced motion: Isolation and dissociation of egocentric and vection-entrained components. *Perception, 20,* 285–305. [PubMed]

Hiris, E., & Blake, R. (1996). Direction repulsion in motion transparency. *Visual Neuroscience, 13,* 187–197. [PubMed]

Holliday, I. E., & Meese, T. S. (2005). Neuromagnetic evoked responses to complex motions are greatest for expansion. *International Journal of Psychophysiology, 55,* 145–157. [PubMed]

Kaminiarz, A., Krekelberg, B., & Bremmer, F. (2007). Localization of visual targets during optokinetic eye movements. *Vision Research, 47,* 869–878. [PubMed]

Koenderink, J. J. (1988). Operational significance of receptive field assemblies. *Biological Cybernetics, 58,* 163–171. [PubMed]

Koenderink, J. J., & van Doorn, A. J. (1987). Facts on optic flow. *Biological Cybernetics, 56,* 247–254. [PubMed]

Lappe, M., Bremmer, F., & van den Berg, A. V. (1999). Perception of self-motion from visual flow. *Trends in Cognitive Sciences, 3,* 329–336. [PubMed]

Lappe, M., & Duffy, C. J. (1999). Optic flow illusion and single neuron behaviour reconciled by a population model. *European Journal of Neuroscience, 11,* 2323–2331. [PubMed]

Lappe, M., & Grigo, A. (1999). How stereovision interacts with optic flow perception: Neural mechanisms. *Neural Networks, 12,* 1325–1329. [PubMed]

Lappe, M., & Rauschecker, J. P. (1995a). An illusory transformation in a model of optic flow processing. *Vision Research, 35,* 1619–1631. [PubMed]

Lappe, M., & Rauschecker, J. P. (1995b). Motion anisotropies and heading detection. *Biological Cybernetics, 72,* 261–277. [PubMed]

Lee, B., Pesaran, B., & Andersen, R. A. (2007). Translation speed compensation in the dorsal aspect of the medial superior temporal area. *Journal of Neuroscience, 27,* 2582–2591. [PubMed] [Article]

Longuet-Higgins, H. C., & Prazdny, K. (1980). The interpretation of a moving retinal image. *Proceedings of the Royal Society of London B, Biological Sciences, 208,* 385–397. [PubMed]

Lott, L. A., & Post, R. B. (1993). Up-down asymmetry in vertical induced motion. *Perception, 22,* 527–535. [PubMed]

MacAvoy, M. G., Gottlieb, J. P., & Bruce, C. J. (1991). Smooth-pursuit eye movement representation in the primate frontal eye field. *Cerebral Cortex, 1,* 95–102. [PubMed]

Mack, A., & Herman, E. (1978). The loss of position constancy during pursuit eye movements. *Vision Research, 18,* 55–62. [PubMed]

Marshak, W., & Sekuler, R. (1979). Mutual repulsion between moving visual targets. *Science, 205,* 1399–1401. [PubMed]

Meese, T. S., Smith, V., & Harris, M. G. (1995). Induced motion may account for the illusory transformation of optic flow fields found by Duffy and Wurtz. *Vision Research, 35,* 981–985. [PubMed]

Moore, T., & Armstrong, K. M. (2003). Selective gating of visual signals by microstimulation of frontal cortex. *Nature, 421,* 370–373. [PubMed]

Moore, T., & Fallah, M. (2004). Microstimulation of the frontal eye field and its effects on covert spatial attention. *Journal of Neurophysiology, 91,* 152–162. [PubMed] [Article]

Morrone, M. C., Tosetti, M., Montanaro, D., Fiorentini, A., Cioni, G., & Burr, D. C. (2000). A cortical area that responds specifically to optic flow, revealed by fMRI. *Nature Neuroscience, 3,* 1322–1328. [PubMed] [Article]

Murakami, I. (1999). Motion-transparent inducers have different effects on induced motion and motion capture. *Vision Research, 39,* 1671–1681. [PubMed]

Murakami, I., & Shimojo, S. (1993). Motion capture changes to induced motion at higher luminance contrasts, smaller eccentricities, and larger inducer sizes. *Vision Research, 33,* 2091–2107. [PubMed]

Mussap, A. J., & Prins, N. (2002). On the perceived location of global motion. *Vision Research, 42,* 761–769. [PubMed]

Newsome, W. T., Wurtz, R. H., & Komatsu, H. (1988). Relation of cortical areas MT and MST to pursuit eye movements. II. Differentiation of retinal from extraretinal inputs. *Journal of Neurophysiology, 60,* 604–620. [PubMed]

Pack, C., & Mingolla, E. (1998). Global induced motion and visual stability in an optic flow illusion. *Vision Research, 38,* 3083–3093. [PubMed]

Perge, J. A., Borghuis, B. G., Bours, R. J., Lankheet, M. J., & van Wezel, R. J. (2005). Dynamics of directional selectivity in MT receptive field centre and surround. *European Journal of Neuroscience, 22,* 2049–2058. [PubMed]

Peuskens, H., Sunaert, S., Dupont, P., Van Hecke, P., & Orban, G. A. (2001). Human brain regions involved in heading estimation. *Journal of Neuroscience, 21,* 2451–2461. [PubMed] [Article]

Post, R. B. (1986). Induced motion considered as a visually induced oculogyral illusion. *Perception, 15,* 131–138. [PubMed]

Post, R. B., & Heckmann, T. (1986). Induced motion and apparent straight ahead during prolonged stimulation. *Perception & Psychophysics, 40,* 263–270. [PubMed]

Post, R. B., Shupert, C. L., & Leibowitz, H. W. (1984). Implications of OKN suppression by smooth pursuit for induced motion. *Perception & Psychophysics, 36,* 493–498. [PubMed]

Ptito, M., Kupers, R., Faubert, J., & Gjedde, A. (2001). Cortical representation of inward and outward radial motion in man. *Neuroimage, 14,* 1409–1415. [PubMed]

Ramachandran, V. S. (1987). Interaction between colour and motion in human vision. *Nature, 328,* 645–647. [PubMed]

Ramachandran, V. S., & Anstis, S. M. (1990). Illusory displacement of equiluminous kinetic edges. *Perception, 19,* 611–616. [PubMed]

Rauber, H. J., & Treue, S. (1999). Revisiting motion repulsion: Evidence for a general phenomenon? *Vision Research, 39,* 3187–3196. [PubMed]

Reinhardt-Rutland, A. H. (1988). Induced movement in the visual modality: An overview. *Psychological Bulletin, 103,* 57–71. [PubMed]

Rieger, J. H., & Toet, L. (1985). Human visual navigation in the presence of 3-D rotations. *Biological Cybernetics, 52,* 377–381. [PubMed]

Royden, C. S., Banks, M. S., & Crowell, J. A. (1992). The perception of heading during eye movements. *Nature, 360*, 583–585. [PubMed]

Royden, C. S., & Conti, D. M. (2003). A model using MT-like motion-opponent operators explains an illusory transformation in the optic flow field. *Vision Research, 43*, 2811–2826. [PubMed]

Rutschmann, R. M., Schrauf, M., & Greenlee, M. W. (2000). Brain activation during dichoptic presentation of optic flow stimuli. *Experimental Brain Research, 134,* 533–537. [PubMed]

Saito, H., Yukie, M., Tanaka, K., Hikosaka, K., Fukada, Y., & Iwai, E. (1986). Integration of direction signals of image motion in the superior temporal sulcus of the macaque monkey. *Journal of Neuroscience, 6,* 145–157. [PubMed] [Article]

Schall, J. D. (2004). On the role of frontal eye field in guiding attention and saccades. *Vision Research, 44,* 1453–1467. [PubMed]

Shenoy, K. V., Bradley, D. C., & Andersen, R. A. (1999). Influence of gaze rotation on the visual response of primate MSTd neurons. *Journal of Neurophysiology, 81,* 2764–2786. [PubMed] [Article]

Shenoy, K. V., Crowell, J. A., & Andersen, R. A. (2002). Pursuit speed compensation in cortical area MSTd. *Journal of Neurophysiology, 88,* 2630–2647. [PubMed] [Article]

Souman, J. L., Hooge, I. T., & Wertheim, A. H. (2005). Vertical object motion during horizontal ocular pursuit: Compensation for eye movements increases with presentation duration. *Vision Research, 45,* 845–853. [PubMed]

Spillmann, L., & Redies, C. (1981). Random-dot motion displaces Ehrenstein illusion. *Perception, 10,* 411–415. [PubMed]

Stanton, G. B., Bruce, C. J., & Goldberg, M. E. (1995). Topography of projections to posterior cortical areas from the macaque frontal eye fields. *Journal of Comparative Neurology, 353,* 291–305. [PubMed]

Tadin, D., Lappin, J. S., & Blake, R. (2006). Fine temporal properties of center-surround interactions in motion revealed by reverse correlation. *Journal of Neuroscience, 26,* 2614–2622. [PubMed] [Article]

Tanaka, K., Hikosaka, K., Saito, H., Yukie, M., Fukada, Y., & Iwai, E. (1986). Analysis of local and wide-field movements in the superior temporal visual areas of the macaque monkey. *Journal of Neuroscience, 6,* 134–144. [PubMed] [Article]

Thompson, K. G., Biscoe, K. L., & Sato, T. R. (2005). Neuronal basis of covert spatial attention in the frontal eye field. *Journal of Neuroscience, 25,* 9479–9487. [PubMed] [Article]

Tian, J. R., & Lynch, J. C. (1996a). Corticocortical input to the smooth and saccadic eye movement subregions of the frontal eye field in Cebus monkeys. *Journal of Neurophysiology, 76,* 2754–2771. [PubMed]

Tian, J. R., & Lynch, J. C. (1996b). Functionally defined smooth and saccadic eye movement subregions in the frontal eye field of Cebus monkeys. *Journal of Neurophysiology, 76,* 2740–2753. [PubMed]

Tozzi, A., Morrone, M. C., & Burr, D. C. (2007). The effect of optokinetic nystagmus on the perceived position of briefly flashed targets. *Vision Research, 47,* 861–868. [PubMed]

van den Berg, A. V. (1996). Judgements of heading. *Vision Research, 36,* 2337–2350. [PubMed]

Warren, W., & Hannon, D. (1988). Direction of self-motion is perceived from optical flow. *Nature, 336,* 162–163.

Warren, W. H., Jr., & Hannon, D. J. (1990). Eye movements and optical flow. *Journal of the Optical Society of America A, Optics and Image Science, 7,* 160–169. [PubMed]

Zhang, T., Heuer, H. W., & Britten, K. H. (2004). Parietal area VIP neuronal responses to heading stimuli are encoded in head-centered coordinates. *Neuron, 42,* 993–1001. [PubMed] [Article]

Zipser, D., & Andersen, R. A. (1988). A back-propagation programmed network that simulates response properties of a subset of posterior parietal neurons. *Nature, 331,* 679–684. [PubMed]